Scattering of electromagnetic waves by periodic structures

1992 J. Phys.: Condens. Matter 4 7389

(http://iopscience.iop.org/0953-8984/4/36/013)

J. Phys.: Condens. Matter 4 (1992) 7389–7400. Printed in the UK

Scattering of electromagnetic waves by periodic structures

N Stefanou†, V Karathanos‡ and A Modinos‡

† Solid State Section, University of Athens, Panepistimioupolis, New Buildings, GR-157 84, Athens, Greece

‡ Department of Physics, National Technical University of Athens, Zografou Campus, GR-157 73, Athens, Greece

Received 12 May 1992

Abstract. We consider periodic structures made of spheres embedded in a host material with a different dielectric function. We show how to calculate the reflection and transmission of electromagnetic waves by a slab of the material parallel to a given crystallographic plane. The method of calculation is based on a doubling-layer scheme which obtains the reflection and transmission matrix elements for the multilayer from those of a single layer. The reflection and transmission characteristics of the slab are related to the complex band structure of the photon field associated with the given crystallographic plane of the corresponding infinite crystal, which is introduced in the manner of the low-energy electron diffraction theory. We present numerical results which demonstrate the applicability of the method to real systems of current interest and point out some interesting physics which arose from our calculations. We show in particular that the non-degenerate bands of the photon field at the centre of the surface Brillouin zone do not couple to the incident radiation, leading to total reflection at normal incidence.

1. Introduction

The optical properties of films consisting of small metallic particles, of approximate radius 100 Å, embedded in a dielectric host material (the composite medium is often called a cermet) are of interest for a variety of reasons, not least of which are possible technological applications, e.g. in the coating of solar energy absorbers [1]. Theoretical treatments of this problem based on the Maxwell Garnett [2] theory and extensions of it [3] fail when the interparticle distance becomes comparable with the wavelength of the incident radiation. When this is the case or when the fractional volume occupied by the metallic particles exceeds 50% or so, a proper solution to Maxwell's equations becomes necessary. Lamb *et al* [4] showed that the eigenmodes of the electromagnetic (EM) field (propagating monochromatic waves) in the composite medium can be calculated by Korringa–Kohn–Rostoker (KKR) methods, the problem being analogous to the calculation of the energy band structure of electrons in ordinary crystals. When the particles distributed in the host material of the composite medium are not identical and/or the arrangement of the particles in space is not periodic, the calculation is complicated further for the same reasons as in the corresponding electronic problem [4]. However, in many cases, when the disorder is weak, a good approximation can be obtained through an effective crystal appropriately defined as in the average T-matrix (ATA) [5] or the coherent-potential approximation (CPA) methods [6].

0953-8984/92/367389+12$04.50

More recently, interest has focused on the optical properties of materials, consisting of spheres in a host material with a different dielectric function, following the suggestion by Yablonovitch [7] that such systems may have important technological applications. These would arise, according to Yablonovitch, from the existence of gaps in the eigenfrequency spectrum of the EM field within such a crystal, which in turn would mean that spontaneous emission would not be possible in such an environment. He pointed out the importance of this phenomenon in relation to many semiconductor devices and he proceeded to demonstrate the reality of EM (so-called photonic) gaps in crystalline composites by actually constructing such a crystal [8].

Calculations of the eigenmodes (frequency band structure) of the EM field in a crystalline structure have been presented by a number of workers [9] based on a plane-wave expansion of the EM field in the medium. These calculations are very useful in so far as they demonstrate the existence or otherwise of photonic gaps in a particular structure but they do not describe an actual experiment, i.e. the reflection and transmission of light by a slab of the material. In the present paper we show how this can be done in a relatively straightforward manner using the mathematical concepts of low-energy electron diffraction (LEED) theory. These are the photonic complex band structure associated with a given surface (crystallographic plane) of the composite crystal, and the doubling-layer method for the evaluation of the reflection and transmission matrix elements of a multilayer of the composite material beginning from those of a single layer.

In our earlier work [10, 11] we have shown how to calculate the matrix elements describing the scattering of EM waves by a plane of spheres. In section 2 of the present paper we show how these can be used to calculate the photonic complex band structure associated with a given surface of the crystal and in the calculation of scattering by multilayers. In section 3 we demonstrate the applicability of the method by applying it to specific examples and point out some interesting physics made apparent after our calculations.

2. Theory

In our previous article [11] we have derived explicit expressions for the matrix elements which describe the scattering of a plane EM wave by a single layer of spheres. The spheres are centred on the sites $\{R_n\}$ of a two-dimensional lattice in the x–y plane, i.e.

$$R_n = n_1 a_1 + n_2 a_2 \tag{1}$$

where a_1 and a_2 are primitive vectors in the x–y plane and $n_1, n_2 = 0, \pm 1, \pm 2, \ldots$. We assume that the spheres which do not overlap each other have the same radius S and permittivity $\epsilon_M(\omega)$.

A plane EM wave incident on the layer of spheres is characterized by its frequency ω and its wavevector $q_\| = k_\| + g$, where $k_\|$ is a reduced wavevector in the surface Brillouin zone (SBZ) of the two-dimensional reciprocal lattice of (1) and g is one of the reciprocal vectors of this lattice. We may, therefore, write the incident plane wave as

$$[E_{\rm in}]^s_{gi} \exp[\mathrm{i} K^s_g \cdot r] \tag{2}$$

$$K^{\pm}_g \equiv (k_\| + g, \pm[\kappa^2 - (k_\| + g)^2]^{1/2}) \tag{3}$$

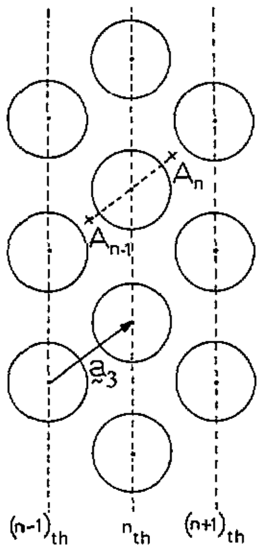

Figure 1. A composite crystal as a stack of successive layers parallel to a crystallographic plane.

where $\kappa = (\mu_0 \epsilon)^{1/2}\omega$ is the wavenumber and we have assumed that the permeability equals the permeability μ_0 of vacuum. We omit the time factor $\exp(-i\omega t)$ and imply, as usual, that the actual field is the real part of the written quantity. We shall also omit writing the associated magnetic field. The three components of the electric field vector $i = x, y, z$ are determined from the magnitude and the polarization direction of the field associated with the given beam g. The superscript $s = +$ or $-$ corresponds to a wave incident on the scatterers from the left or from the right respectively.

In what follows the incident field is usually a sum of terms (2) corresponding to various g beams but of the same $k_{\|}$ and ω. The corresponding scattered wave is also a superposition of plane waves, each of which can be written as

$$[E_{\rm sc}]^s_{gi} \exp[iK^s_g \cdot r] \tag{4}$$

where the $s = +$ and $s = -$ sign on K are used for $z > 0$ and $z < 0$, respectively. We have

$$[E_{\rm sc}]^s_{gi} = \sum_{g',i'} M^{ss'}_{gi;g'i'} [E_{\rm in}]^{s'}_{g'i'} \tag{5}$$

which define the scattering matrix elements $M^{ss'}_{gi;g'i'}$. Explicit expressions for these elements have been given in [11].

2.1. *Photonic complex band structure*

A multilayer is constituted as a stack of identical layers parallel to the x–y plane, so that the $(n+1)$th layer along the positive z direction is obtained from the nth layer by a simple translation described by a vector a_3 (figure 1). When the stack of layers extends over all space (from $z = -\infty$ to $z = \infty$), we have an infinite crystal and $\{a_1, a_2, a_3\}$ is a set of primitive vectors for this crystal.

The reduced $\boldsymbol{k}$ zone of the corresponding reciprocal space is $(\boldsymbol{k}_{\|}, k_z)$ where $\boldsymbol{k}_{\|} = (k_x, k_y)$ extends over the SBZ of the plane under consideration and $-|\boldsymbol{b}_3|/2 < k_z \leqslant |\boldsymbol{b}_3|/2$ where $\boldsymbol{b}_3 \equiv 2\pi \boldsymbol{a}_1 \times \boldsymbol{a}_2 / \boldsymbol{a}_1 \cdot (\boldsymbol{a}_2 \times \boldsymbol{a}_3)$. The complex band structure of the EM field associated with the given surface is obtained in the same manner as for the Schrödinger wave field of electrons in an ordinary crystal. The eigenmodes are in both cases generalized Bloch waves of frequency ω and reduced wavevector $\boldsymbol{k}_{\|}$ parallel to the surface.

In the region of host space between the nth and the $(n+1)$th layers of spheres the wave field of given ω and $\boldsymbol{k}_{\|}$ has the form

$$\sum_{\boldsymbol{g}} \left\{ \boldsymbol{E}_{\boldsymbol{g}}^{+}(n) \exp[\mathrm{i}\boldsymbol{K}_{\boldsymbol{g}}^{+} \cdot (\boldsymbol{r} - \boldsymbol{A}_n)] + \boldsymbol{E}_{\boldsymbol{g}}^{-}(n) \exp[\mathrm{i}\boldsymbol{K}_{\boldsymbol{g}}^{-} \cdot (\boldsymbol{r} - \boldsymbol{A}_n)] \right\} \tag{6}$$

where $\boldsymbol{A}_n$ is the midpoint between the nth and the $(n+1)$th layer (see figure 1).

The vector coefficients $\boldsymbol{E}_{\boldsymbol{g}}^{\pm}(n)$ are related to the $\boldsymbol{E}_{\boldsymbol{g}}^{\pm}(n+1)$ coefficients through the scattering properties of the nth layer. One can easily see that

$$E_{\boldsymbol{g}i}^{-}(n) = \sum_{\boldsymbol{g}'i'} Q_{\boldsymbol{g}i;\boldsymbol{g}'i'}^{--} E_{\boldsymbol{g}'i'}^{-}(n+1) + \sum_{\boldsymbol{g}'i'} Q_{\boldsymbol{g}i;\boldsymbol{g}'i'}^{-+} E_{\boldsymbol{g}'i'}^{+}(n) \tag{7a}$$

$$E_{\boldsymbol{g}i}^{+}(n+1) = \sum_{\boldsymbol{g}'i'} Q_{\boldsymbol{g}i;\boldsymbol{g}'i'}^{++} E_{\boldsymbol{g}'i'}^{+}(n) + \sum_{\boldsymbol{g}'i'} Q_{\boldsymbol{g}i;\boldsymbol{g}'i'}^{+-} E_{\boldsymbol{g}'i'}^{-}(n+1) \tag{7b}$$

where $i = x, y, z$ and

$$\begin{aligned}
Q_{\boldsymbol{g}i;\boldsymbol{g}'i'}^{--} &= \exp\left[-(\mathrm{i}/2)\left(\boldsymbol{K}_{\boldsymbol{g}}^{-} + \boldsymbol{K}_{\boldsymbol{g}'}^{-}\right) \cdot \boldsymbol{a}_3\right] M_{\boldsymbol{g}i;\boldsymbol{g}'i'}^{--} \\
Q_{\boldsymbol{g}i;\boldsymbol{g}'i'}^{-+} &= \exp\left[-(\mathrm{i}/2)\left(\boldsymbol{K}_{\boldsymbol{g}}^{-} - \boldsymbol{K}_{\boldsymbol{g}'}^{+}\right) \cdot \boldsymbol{a}_3\right] M_{\boldsymbol{g}i;\boldsymbol{g}'i'}^{-+} \\
Q_{\boldsymbol{g}i;\boldsymbol{g}'i'}^{++} &= \exp\left[(\mathrm{i}/2)\left(\boldsymbol{K}_{\boldsymbol{g}}^{+} + \boldsymbol{K}_{\boldsymbol{g}'}^{+}\right) \cdot \boldsymbol{a}_3\right] M_{\boldsymbol{g}i;\boldsymbol{g}'i'}^{++} \\
Q_{\boldsymbol{g}i;\boldsymbol{g}'i'}^{+-} &= \exp\left[(\mathrm{i}/2)\left(\boldsymbol{K}_{\boldsymbol{g}}^{+} - \boldsymbol{K}_{\boldsymbol{g}'}^{-}\right) \cdot \boldsymbol{a}_3\right] M_{\boldsymbol{g}i;\boldsymbol{g}'i'}^{+-}.
\end{aligned} \tag{8}$$

The phase factors in the above equations arise from the fact that the waves in (6) refer to an origin half-way between two successive layers whereas the matrix elements in (5) were calculated with the origin of coordinates at the centre of the layer.

Now it is in the nature of a generalized Bloch wave that

$$\boldsymbol{E}_{\boldsymbol{g}}^{\pm}(n+1) = \exp(\mathrm{i}\boldsymbol{k} \cdot \boldsymbol{a}_3)\, \boldsymbol{E}_{\boldsymbol{g}}^{\pm}(n) \tag{9}$$

$$\boldsymbol{k} = (\boldsymbol{k}_{\|}, k_z(\omega; \boldsymbol{k}_{\|})) \tag{10}$$

where k_z is a function of ω and $\boldsymbol{k}_{\|}$, to be determined for each of the modes of the EM field in the given crystal.

Substitution of equation (9) into equation (7) leads after some algebra, to the following system of equations:

$$\begin{bmatrix} \mathbf{Q}^{++} & \mathbf{Q}^{+-} \\ -[\mathbf{Q}^{--}]^{-1}\mathbf{Q}^{-+}\mathbf{Q}^{++} & [\mathbf{Q}^{--}]^{-1}[\mathbf{I} - \mathbf{Q}^{-+}\mathbf{Q}^{+-}] \end{bmatrix} \begin{bmatrix} \boldsymbol{E}^{+}(n) \\ \boldsymbol{E}^{-}(n+1) \end{bmatrix} = \exp(\mathrm{i}\boldsymbol{k} \cdot \boldsymbol{a}_3) \begin{bmatrix} \boldsymbol{E}^{+}(n) \\ \boldsymbol{E}^{-}(n+1) \end{bmatrix} \tag{11}$$

where $E^{\pm}$ are column vectors with the components $E^{\pm}_{g_1x}$, $E^{\pm}_{g_1y}$, $E^{\pm}_{g_1z}$, $E^{\pm}_{g_2x}$, $E^{\pm}_{g_2y}$, $E^{\pm}_{g_2z}$, ... In practice we keep N g-vectors in the calculation (those of smallest magnitude) in which case $E^{\pm}$ are vectors with $3N$ components. The enumeration of g-vectors implied in the definition of $E^{\pm}$ allows us to write the **Q**-matrix elements in compact form as matrices $\mathbf{Q}^{++}$, $\mathbf{Q}^{+-}$, etc, each of which has $3N \times 3N$ elements; **I** is the $3N \times 3N$ unit matrix. This means that we have in (11) a system of $6N$ homogeneous equations with $6N$ unknowns. Equation (11) is the EM field equivalent to McRae's equation for the Schrödinger wave field of an electron in a crystal [12, 13]. We note that for given $k_{\|}$ and ω we obtain $6N$ eigenvalues of k_z from the solvability condition of equation (11). Looked upon as functions of ω, these define, for each $k_{\|}$, $6N$ different lines $k_z(\omega; k_{\|})$ in the complex k_z-space. The general properties of these real frequency lines (which is what they are called) are known from the corresponding electron problem [14] but will not concern us here. It is sufficient for our purposes to observe that, for given $k_{\|}$ and ω, none or at best very few of the corresponding eigenvalues of k_z are real, the rest being complex. We note that, because the solvability condition of (11) determines a value for $\exp(\mathrm{i}k \cdot a_3)$, values of k_z differing by an integral multiple of $|b_3|$ correspond to the same eigenmode which establishes the required periodicity of the band structure in k-space. We must also bear in mind that only solutions with an associated electric field of zero divergence are of physical interest. One third of the eigensolutions do not satisfy this condition and we drop them. Of the remaining we have a limited number, as we have already mentioned, of propagating waves which correspond to real values of k_z, and the rest are evanescent waves which correspond to complex values of k_z. These have an amplitude which increases exponentially in the positive or negative z direction and do not exist as physical entities in an infinite crystal.

A region of frequencies over which propagating waves do not exist for a given $k_{\|}$ constitutes a frequency gap in the EM field, for the given $k_{\|}$. If the crystal is not infinite (it never is) but of finite extension in the z direction, the transmission of EM waves with ω within a gap is determined essentially by the eigenmode with the smallest imaginary component of k_z.

More important are regions of frequency over which no propagating Bloch waves exist whatever the value of $k_{\|}$. These may be thought of as absolute gaps in the frequency spectrum of the EM field.

We shall comment further on aspects of the complex band structure of the EM field after we present some numerical results in section 3.

2.2. *Scattering of light by multilayers*

Knowledge of the complex band structure of the EM field associated with a given surface of a crystal provides us with the means to calculate the scattering of the EM wave of given ω and $q_{\|} = k_{\|} + g$ from this surface when the crystal occupies the half-space from $z = -\infty$ to $z = 0$. This is achieved by matching the EM field on the vacuum side of the interface ($z > 0$) which consists of the incident plus reflected beams propagating or decaying as $z \to \infty$ to the EM field inside the crystal which we write as a superposition of Bloch waves propagating or decaying away from the surface ($z \to -\infty$). Matching at the interface ($z = 0$) means in this case that the unknown coefficients in the sums which describe the EM field on either side of the interface are determined through the requirement that the tangential component of the electric and magnetic field be continuous across the interface. Otherwise the

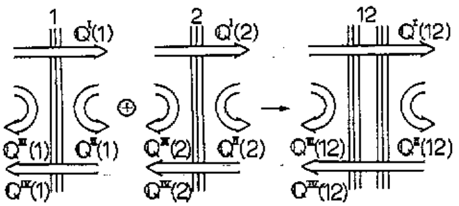

Figure 2. The **Q**-matrix elements for two successive layers are obtained from those of the individual layers (schematic description).

procedure is completely analogous to that in LEED theory.

Similarly we can calculate the transmission and reflection of EM waves through a multilayer, a slab of the crystal infinite in the x–y direction but of finite extension along the z direction. For an EM wave incident from the left, the field on the left-hand side of the slab consists of the incident plus reflected beams. On the right-hand side of the slab the EM field consists of transmitted beams propagating or decaying as $z \to \infty$. Inside the slab it is a superposition of Bloch waves propagating or decaying in either direction. Matching of the EM field at both surfaces of the slab determines the amplitude of the reflected and the transmitted beams.

The above procedure may be efficient when we are dealing with multilayers or indeed with reflection from an infinite crystal. When the multilayer consists of a few layers, as it does in the experiment of Yablonovitch and Gmitter [8], an alternative method [12, 13] may be used to calculate the reflection and transmission matrix elements of the multilayer. The method avoids altogether the calculation of the complex band structure of the EM field and proceeds to the calculation of the matrix elements of the multilayer as follows. We combine the matrix elements of two successive single layers as shown schematically in figure 2 to obtain those of the double layer. The notation used is as follows. The matrices $\mathbf{Q}^{++}$, $\mathbf{Q}^{+-}$, $\mathbf{Q}^{-+}$ and $\mathbf{Q}^{--}$ for the first layer are denoted by $\mathbf{Q}^{\mathrm{I}}(1)$, $\mathbf{Q}^{\mathrm{II}}(1)$, $\mathbf{Q}^{\mathrm{III}}(1)$ and $\mathbf{Q}^{\mathrm{IV}}(1)$, respectively, the corresponding matrices for the second layer are denoted by $\mathbf{Q}^{\mathrm{I}}(2)$, $\mathbf{Q}^{\mathrm{II}}(2)$, etc. All matrices refer of course to the same ω and $k_{\|}$, and the waves are expressed with respect to the origins defined in each region as in figure 1. For example, the waves incident from the left on the double layer refer to an origin which lies where the midpoint would be between the first layer and that preceding it in the corresponding infinite crystal. The details of the method can be found elsewhere [13]. It is easily shown that

$$\begin{aligned}
\mathbf{Q}^{\mathrm{I}}(12) &= \mathbf{Q}^{\mathrm{I}}(2)[\mathbf{I} - \mathbf{Q}^{\mathrm{II}}(1)\mathbf{Q}^{\mathrm{III}}(2)]^{-1}\mathbf{Q}^{\mathrm{I}}(1) \\
\mathbf{Q}^{\mathrm{II}}(12) &= \mathbf{Q}^{\mathrm{I}}(2)\mathbf{Q}^{\mathrm{II}}(1)[\mathbf{I} - \mathbf{Q}^{\mathrm{III}}(2)\mathbf{Q}^{\mathrm{II}}(1)]^{-1}\mathbf{Q}^{\mathrm{IV}}(2) + \mathbf{Q}^{\mathrm{II}}(2) \\
\mathbf{Q}^{\mathrm{III}}(12) &= \mathbf{Q}^{\mathrm{IV}}(1)\mathbf{Q}^{\mathrm{III}}(2)[\mathbf{I} - \mathbf{Q}^{\mathrm{II}}(1)\mathbf{Q}^{\mathrm{III}}(2)]^{-1}\mathbf{Q}^{\mathrm{I}}(1) + \mathbf{Q}^{\mathrm{III}}(1) \\
\mathbf{Q}^{\mathrm{IV}}(12) &= \mathbf{Q}^{\mathrm{IV}}(1)[\mathbf{I} - \mathbf{Q}^{\mathrm{III}}(2)\mathbf{Q}^{\mathrm{II}}(1)]^{-1}\mathbf{Q}^{\mathrm{IV}}(2)
\end{aligned} \tag{12}$$

where the argument 12 refers to the **Q**-matrices of the two layers. It is obvious that we can repeat the process to obtain the matrix elements of four layers, then those of eight layers and so on. We should also emphasize that the method applies equally well (at the expense of further computation) to multilayers constituted from different single layers as long as they have the same periodic structure (that of equation (1)) parallel to the x–y plane.

3. Numerical results and discussion

We calculated the complex band structure of the EM field for the (001) face of a FCC crystal, with lattice constant a, of dielectric spheres (one per lattice site) in vacuum. The non-overlapping spheres with a radius $S = 0.4d$, where $d = a/\sqrt{2}$ denotes the distance between first neighbours, occupy 37.91% of the crystal space. The refractive index of the spheres, $n = 3.06$, is that of polycrystalline Al_2O_3 used in the experiments of Yablonovitch and Gmitter [8].

The M-matrix elements in (5) are obtained through an angular momentum expansion with a cut-off at $l_{\max} = 5$ which gives good convergence [11]. As to the number N of g-vectors required in the description of layer scattering, we find that $N = 9$ yields results accurate to better than 1% in all cases.

We show the real frequency lines for $k_{\|} = (0,0)$, associated with normal incidence, in figure 3, and those for a general point of the SBZ—we have taken $k_{\|} = (2\pi/a)\sqrt{2}$ (0.2, 0.1)—associated with incidence at an angle, in figure 4. We present only those lines which over frequency regions have $k_z(\omega; k_{\|})$ real. These frequency regions constitute the equivalent of the energy bands in the electronic energy band structure of ordinary crystals. We refer to them as frequency bands of the EM field in the composite crystal or, simply, as frequency bands of the photon field. For clarity in the presentation we do not show the complex k_z sections of all the lines in figures 3 and 4. It is not important for our purposes to identify a particular line as it develops in the complex k_z-space with increasing ω. The parts of the complex k_z lines that we show are those which determine the attenuation of the EM field in the respective frequency gaps. The imaginary part of $k_z(\omega; k_{\|})$, shown by dotted curves in the figures, is drawn to the same scale as the rest of the figure. The real part of the complex k_z is not shown. Because the (001) plane is a plane of symmetry of the crystal, the solutions (Bloch waves) appear in pairs: $k_z(\omega; k_{\|})$ and $-k_z(\omega; k_{\|})$; in the figures we show those with $\mathrm{Re}\{k_z(\omega; k_{\|})\} \geqslant 0$. We should also point out that the way that the results are presented—plotting $\omega a/c$, where c is the velocity of light, against $k_z a/2\pi$—renders them applicable to different ranges of frequency of the EM field, provided that the size of the unit cell is scaled accordingly.

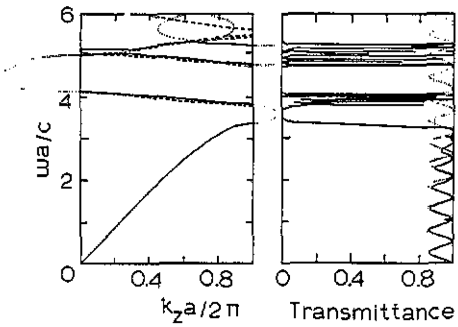

Figure 3. The photonic complex band structure at the centre of the SBZ of a (001) surface of a FCC composite crystal, together with the corresponding transmittance curve of a slab of eight layers parallel to the same surface. The crystal is constituted of spheres of dielectric constant $\epsilon_M = 9.3636$ in vacuum with a volume coverage $b = 0.3791$. The transmittance curve of a homogeneous slab with $\bar{\epsilon} = 2.16$ is shown by the dotted curve.

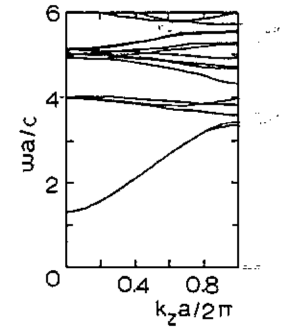

Figure 4. The photonic complex band structure associated with the (001) surface of a FCC composite crystal for $k_\parallel = (2\pi/a)\sqrt{2}$ (0.2, 0.1). The crystal is constituted of spheres of dielectric constant $\epsilon_M = 9.3636$ in vacuum with a volume coverage $b = 0.3791$.

We now comment on the results shown in figures 3 and 5. The lowest band behaves in the long-wavelength limit ($k \to 0$) as we expect. In this limit we can replace the crystal by a uniform medium with an effective dielectric constant $\overline{\epsilon}$ given by [3]

$$(\overline{\epsilon} - \epsilon)/(\overline{\epsilon} + 2\epsilon) = b(\epsilon_M - \epsilon)/(\epsilon_M + 2\epsilon) \tag{13}$$

where b is the fractional volume occupied by the spheres. In our case, $b = 0.3791$, $\epsilon = 1$, $\epsilon_M = 9.3636$ and, therefore, equation (13) gives $\overline{\epsilon} = 2.16$, with a corresponding refractive index $\overline{n} = 1.47$. This means that, for small values of ω and for normal incidence ($k_\parallel = 0$), we should have $c(\mathrm{d}k_z/\mathrm{d}\omega) = \overline{n} = 1.47$, which is indeed what is obtained from figure 3.

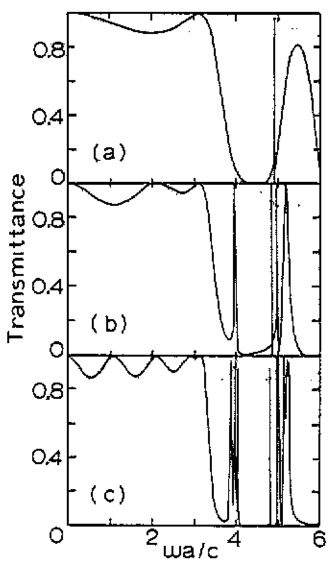

Figure 5. Transmittance versus frequency curves (——) of EM waves incident normally on a slab of (*a*) one, (*b*) two and (*c*) four layers, parallel to the (001) surface of a FCC composite crystal. The crystal is constituted of spheres of dielectric constant $\epsilon_M = 9.3636$ in vacuum with a volume coverage $b = 0.3791$. The transmittance of the corresponding homogeneous slabs with $\overline{\epsilon} = 2.16$ is shown by dotted curves.

Of the frequency bands in figure 3, four, shown by full curves, are doubly degenerate (Δ_5 symmetry) and correspond to two different, mutually orthogonal polarizations of the electric field. The remaining six bands, shown by broken curves, are non-degenerate and of Δ_1, Δ_2, Δ'_1, Δ'_2-type symmetry. Whatever the symmetry of the non-degenerate bands, the $g = \mathbf{0}$ component of the corresponding eigenmodes of the EM field (the Bloch waves described by (6)) vanishes. Non-degeneracy and the transverse nature of the EM field demand that this be so for any one of these symmetries. This has an important consequence in relation to scattering of plane waves incident normally on a slab of the crystal. Because the $g = \mathbf{0}$ beam is the only one which matches a propagating wave outside the crystal, the incident wave cannot excite an internal mode with a vanishing $g = \mathbf{0}$ component, and the incident wave will be totally reflected; there will be no transmission of light through the slab, assuming of course that no other bands with a non-vanishing $g = \mathbf{0}$ component exist at the given frequency. This is the case for the top band in figure 3 and the same applies to the top sections of the two bands immediately below the top band. This is shown clearly in figure 3 where the transmittance of light incident normally on a slab of eight layers is plotted versus frequency. It is seen there that no light is transmitted through the slab when $a\omega/c > 5.3$. We note that the symmetry argument breaks down when $k_\parallel \neq \mathbf{0}$, and transmission increases gradually with light incident at an angle. This can be seen from figures 4 and 6. It may be that the phenomenon of rigorously vanishing transmittance when light is incident normally on a given surface can be of use in technological applications, apart from being an interesting phenomenon in itself. The Δ_5 bands (full curves in figure 3) couple to incident EM waves. We see in figure 3 that, when an EM wave is incident normally on a slab of eight layers, it is almost totally transmitted through the slab if the frequency lies within one or the other of the Δ_5 bands and almost totally reflected when its frequency lies within a frequency gap. It is evident (see also figure 5) that the discreteness of the transmission spectrum for $\omega a/c > 3$ is replaced by an almost continuous spectrum as the thickness (number of layers in the slab) increases. We note that the two eigenmodes of the doubly degenerate Δ_5 band couple respectively to the two different, mutually orthogonal polarizations of the incident field, leading to identical transmission spectra for the two polarization directions.

The oscillations of the transmission coefficient shown in figure 3 in the lower-frequency range of the spectrum where an effective-medium approximation is more or less valid result from interference between the waves reflected at the two surfaces of the slab and are well understood [15]. In the same figure we show by a dotted curve the transmittance evaluated for a corresponding homogeneous slab with $\bar{\epsilon} = 2.16$ and thickness given by the number of layers times the z component of a_3 (see figure 1). We see the agreement in the lower-energy range of the spectrum. The disagreement in the higher-frequency range is also evident.

In figure 5 we show the transmission spectra for slabs which are one layer, two layers and four layers thick. It is clear that for these thinner slabs the frequency bands of the infinite crystal provide only a rough guide to the transmission spectrum, and yet it is remarkable that the transmittance of two layers or even that of one layer exhibits features which can be understood in terms of the photonic complex band structure of the infinite crystal. We note in particular that transmission through the slab when the frequency of the incident wave lies within a frequency gap is determined by the imaginary component of $k_z(\omega; k_\parallel)$ and is therefore larger when $\mathrm{Im}\{k_z(\omega; k_\parallel)\}$ is smaller. This can be seen quite clearly in the case of the two-layer slab. In the gap immediately below $\omega a/c \simeq 4$, the imaginary component of k_z is on the average smaller than in the corresponding gap above $\omega a/c \simeq 4$ as shown in figure 3, and therefore we expect transmission over the frequency range of the lower gap to be

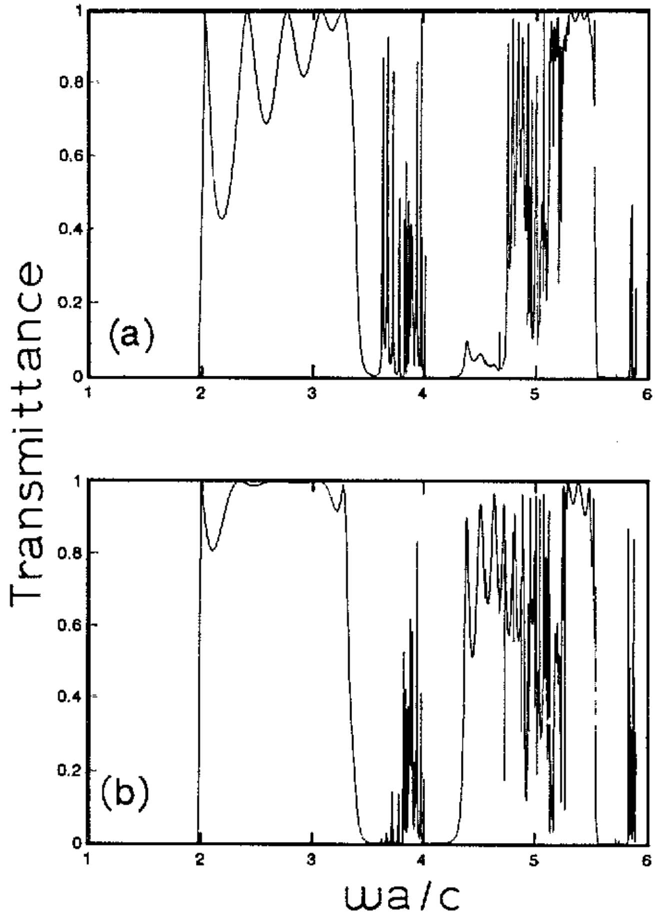

Figure 6. Transmittance versus frequency curves of EM waves incident on a slab of eight layers parallel to the (001) surface of a FCC composite crystal with $k_{\|} = (2\pi/a)\sqrt{2}$ (0.2, 0.1) for (*a*) s and (*b*) p polarization. The crystal is constituted of spheres of dielectric constant $\epsilon_M = 9.3636$ in vacuum with a volume coverage $b = 0.3791$.

larger than that of the higher-frequency gap. This is indeed the case as can be seen in figure 5. For a four-layer slab, transmission is reduced to zero in the higher-frequency gap, but not so in the lower gap where it is small but certainly not negligible. For comparison the transmittance of the corresponding homogeneous slabs with $\bar{\epsilon} = 2.16$ is also shown in figure 5 by the dotted curves.

Let us now comment briefly on our results in relation to light incident at an angle on the (001)-faced slab of our composite crystal. The complex band structure for the chosen point in the SBZ, $k_{\|} = (2\pi/a)\sqrt{2}$ (0.2, 0.1), is shown in figure 4. None of the bands is degenerate and none can be described as s or p polarized in the sense usually given to these expressions, meaning a well defined polarization direction of the associated electric field (in the surface of the slab for s, and in the plane of incidence for p polarization). The imaginary part of $k_z(\omega; k_{\|})$ of the important real frequency lines (those which determine the attenuation of light in the slab) is shown by dotted curves over the frequency range of their respective frequency gaps.

The lowest eigenfrequency ω_0 for the given $k_\parallel$ can be estimated assuming that the effective-medium approximation is valid as $k_z \to 0$. We then have $\omega_0 = (c/\overline{n})k_\parallel$. Substituting for $\overline{n}$ the previously found value ($\overline{n} = 1.47$) we find that $\omega_0 a/c = 1.35$, which lies very near the value of $\omega_0 a/c = 1.33$, obtained from figure 4.

We show the transmission coefficient of s-polarized light as a function of frequency for the given $k_\parallel$ in figure 6(*a*), and the corresponding spectrum for p-polarized light in figure 6(*b*). Firstly we note the considerable transmission above $a\omega/c = 5.3$, where there was none for normal incidence, the origin of which we have already explained. Then we observe that the oscillations of the transmittance curve in the lower-energy part of the spectrum are different for s- and p-polarized light, which again is what one expects from traditional effective-medium theory. Finally, we observe that for incidence at an angle the transmittance curves are much more complicated than in the case of normal incidence. We cannot now say that the transmission coefficient equals unity if the frequency of the incident wave lies within one of the frequency bands. Knowledge of the frequency bands does not by itself determine the transmission coefficient in the present case. For example we note that an s-polarized wave transmits only to a small extent in the $\omega a/c$ range from 4.3 to 4.7, whereas a p-polarized wave transmits to a much larger extent over the same region of frequencies.

4. Conclusion

In conclusion, we may say that, in order to analyse fully the results of experiments relating to the reflection and transmission of EM waves by slabs of composite crystals, we need to go beyond the calculation of the frequency bands of the EM field in the crystal. It is not necessary to calculate the complex band structure in each case as we have done here. It is sufficient to calculate the reflection and transmission matrices of the slab, and we have shown how this can be done when the slab consists of identical layers. However, knowing the complex band structure of the EM field is always helpful in the interpretation of one's results. We pointed out the interesting phenomenon of vanishing transmittance for normal incidence, when the corresponding frequency band in the crystal is non-degenerate. Finally, we should say that the method that we described applies equally well, when the dielectric function of the spheres or the host space varies with the frequency (the spheres can be metallic for example). Also the doubling-layer method can be easily extended to the case when successive layers are different from each other, as long as they have the same periodic arrangement in the plane of the surface.

References

[1] Sievers A J 1979 *Solar Energy Conversion* ed B O Seraphin (Berlin: Springer) p 57

[2] Maxwell Garnett J C 1904 *Phil. Trans. R. Soc.* A **203** 385; 1906 *Phil. Trans. R. Soc.* A **205** 237

[3] Abeles F, Borensztein Y and Lopez-Rios T 1984 *Festkörperprobleme (Advances in Solid State Physics)* vol XXIV (Braunschweig: Vieweg) p 93

[4] Lamb W, Wood D M and Ashcroft N W 1980 *Phys. Rev.* B **21** 2248

[5] Stefanou N and Modinos A 1991 *J. Phys.: Condens. Matter* **3** 8149

[6] Liebsch A and Persson B N J 1983 *J. Phys. C: Solid State Phys.* **16** 5375
Persson B N J and Liebsch A 1983 *Phys. Rev.* B **28** 4247

[7] Yablonovitch E 1987 *Phys. Rev. Lett.* **58** 2059

[8] Yablonovitch E and Gmitter T J 1989 *Phys. Rev. Lett.* **63** 1950
[9] Leung K M and Liu Y F 1990 *Phys. Rev. Lett.* **65** 2646
Zhang Z and Sapathy S 1990 *Phys. Rev. Lett.* **65** 2650
Ho K M, Chan C T and Soukoulis C M 1990 *Phys. Rev. Lett.* **65** 3152
[10] Modinos A 1987 *Physica* A **141** 575
[11] Stefanou N and Modinos A 1991 *J. Phys.: Condens. Matter* **3** 8135
[12] Pendry J B 1974 *Low Energy Electron Diffraction* (London: Academic) p 138
[13] Modinos A 1984 *Field, Thermionic, and Secondary Electron Emission Spectroscopy* (New York: Plenum) p 136
[14] Heine V 1963 *Proc. Phys. Soc.* **81** 300
[15] Born M and Wolf E 1975 *Principles of Optics* (Oxford: Pergamon) p 51